NBSIR 86-3377

The Effect of Interior Mass Surfaces on the Space Heating and Cooling Loads of A Single-Family Residence

D.M. Burch
G.N. Walton
K. Cavanaugh
B.A. Licitra

U.S. DEPARTMENT OF COMMERCE
National Bureau of Standards
Gaithersburg, MD 20899

June 1986

Prepared for:
Department of Energy

and

Electric Power Research Institute

NBSIR 86-3377

THE EFFECT OF INTERIOR MASS SURFACES ON THE SPACE HEATING AND COOLING LOADS OF A SINGLE-FAMILY RESIDENCE

D.M. Burch
G.N. Walton
K. Cavanaugh
B.A. Licitra

U.S. DEPARTMENT OF COMMERCE
National Bureau of Standards
Gaithersburg, MD 20899

June 1986

Prepared for:
Department of Energy

and

Electric Power Research Institute

U.S. DEPARTMENT OF COMMERCE, Malcolm Baldrige, *Secretary*
NATIONAL BUREAU OF STANDARDS, Ernest Ambler, *Director*

Contents

THE EFFECT OF INTERIOR MASS SURFACES ON THE SPACE HEATING AND COOLING LOADS OF A SINGLE-FAMILY RESIDENCE

D. M. Burch, G. N. Walton, K. Cavanaugh, and B. A. Licitra

ABSTRACT

A Computer Program called TARP is used to analyze the effect of interior mass surfaces (i.e., partition walls and interior furnishings) on the weekly space heating and cooling loads of an insulated and a poorly insulated residence.

In space heating applications, when the outdoor temperature deviated from the balance point, the inclusion of interior mass surfaces in the modeling of the houses increased the interior radiant temperature. This, in turn, increased the overall envelope heat-transfer coefficients of the houses. This effect was found to be more significant in the poorly insulated house compared to the insulated house. When the outdoor temperature was near the balance point, the thermal storage provided by interior surfaces caused the internal heat gains to be more effectively utilized, and weekly space heating loads tended to approach a "high mass limit" that coincided with steady-state theory. Under this condition, additional mass has only a small effect on space heating loads.

In space cooling applications, the inclusion of interior surfaces increased the "effective envelope heat-transfer coefficient" in a linear regime away from the balance point, but produced little change in space cooling loads in a nonlinear regime near the balance point. Thermal insulation in the building envelope was found to have a small effect in reducing annual space cooling loads.

The results of this study indicated that errors can occur when interior mass surfaces are excluded from dynamic computer simulations of residences.

INTRODUCTION

The National Bureau of Standards recently carried out field studies using six one-room test cells in Gaithersburg, MD to investigate the effect of wall mass on space heating and cooling loads. The test cells were extensively instrumented, and their space heating and cooling loads were monitored over a one-year period. The results of these studies were reported separately for space heating loads (Burch, Krintz, and Spain 1984) and space cooling loads (Burch, Davis, and Malcolm 1984). The study pertaining to space heating found that wall mass did not have a measurable effect on space heating loads during the cold part of the winter. However, during mild spring heating days, when the internal heat gains caused the indoor temperature to rise above the thermostat setpoint temperature, a significant thermal mass effect was observed. The heavyweight masonry and log buildings consumed less space heating energy than identical lightweight buildings having equivalent thermal resistance in their building envelopes. Wall mass was found to be more effective when it was placed inside, as opposed to outside, the wall insulation. The study pertaining to space cooling found that wall mass of

---

D. M. Burch and G. N. Walton are mechanical engineers, K. Cavanaugh is an engineering student, and B. A. Licitra is a computer programmer; Center for Building Technology, National Bureau of Standards.

these test buildings had a significant effect on space cooling loads during the entire summer season of Gaithersburg, MD.

While the field study results conclusively demonstrated the existence of a thermal mass effect, they were found to have limited applicability to real houses because the test cells were small, the solar gains through windows were small, and the top surfaces of the floors were insulated.

A limited series of tests was conducted with a partition wall installed in two of the test cells. These tests are described in the appendix. However, both the field measurements and computer predictions indicated that the effect of a partition wall in these test cells was very small. This was because direct solar gain through windows did not enter the test cells during periods when a thermal mass effect would normally be expected. For this reason, these partition wall tests were believed not to be directly applicable to residential buildings.

This study investigates the predicted effect of interior mass features on weekly space heating and cooling loads in an insulated and a poorly insulated single-family residence under more realistic conditions of solar gain through windows.

DESCRIPTION OF COMPUTER PROGRAM

The Thermal Analysis Reseach Program (TARP) is a computer program that predicts either the indoor temperature or space heating/cooling loads of a building under a dynamic set of boundary conditions. TARP uses a detailed heat-balance method to determine heating/cooling requirements from the predicted heat losses and heat gains. The computer algorithms are partly based on subroutines from the Building Loads Analysis and System Thermodynamics (BLAST) Computer Program. In using TARP, a detailed description of the building including the heat-transfer parameters for all materials comprising the building envelope, an operation schedule for the building, and hourly outdoor climatic data are specified as input for the program. Further information on TARP may be found in (Walton 1980).

Space heating and cooling loads predicted by TARP were compared to corresponding measured space heating and cooling loads for the six thermal mass test cells with good agreement in (Burch, Walton, Cavanaugh, and Licitra 1984). In these comparisons, TARP predictions accurately followed the general trends of the measured data. TARP predicted peak space heating and cooling loads within 15% and 18%, respectively. This level of agreement was considered to be reasonable in view of the uncertainty in the heat-transfer properties of the building materials specified as input for the program and the simplifying approximations in the computer algorithms. The level of agreement is comparable and in most cases better than that for other similar computer programs cited in the literature (Arumi-Noe 1984, Burch et al. 1975, Judkoff et al. 1983, and Anderson et al. 1980). A strong case for the validity of the TARP program relative to the thermal mass studies (Burch, Krintz, and Spain 1984 and Burch, Davis, and Malcolm 1984) is that during climatic periods when a thermal mass effect was experimentally observed, the TARP program predicted the correct relative cumulative space conditioning loads. That is, the ranking of the test cells and the relative magnitudes of the predicted thermal mass effects were the same as those for the actual test cells.

DESCRIPTION OF HOUSES USED IN THE ANALYSIS

The geometric design of the two houses used in the computer analysis was fashioned

after the Hastings' ranch house (Hastings 1977). The houses were wood-frame ramblers having a floor area of 1180 ft^2 (110 m^2). They had a pitched roof and ventilated attic. The wall construction consisted of 2 x 4 in (50 x 100 mm) framing placed 16 in (0.41 m) on center with wood siding and gypsum board attached to exterior and interior surfaces, respectively. The windows had a surface area of 141 ft^2 (13.1 m^2), or 12% of the floor area. For each orientation, the ratio of window area to gross wall area was constant. The floor consisted of 1 in (2.5 cm) wood covered with carpet placed over a ventilated crawlspace. A floor plan and elevation are given in Figure 1.

Using the above basic geometric design, an insulated house and a poorly insulated house were considered as separate cases. The basic features of these two houses are given in Table 1. Heat-transfer parameters are given in Table 2 for the insulated house and in Table 3 for the poorly insulated house.

MODELING THE HOUSES

The houses were simulated as three zones including a living space, an attic, and a crawlspace. Space conditioning was provided in the living space. Partition walls and interior furnishings were included as separate surfaces within the living space. The air temperature within each zone was treated as being uniform at each time step of the analysis. The radiant interchange among the surfaces within each zone was computed by the mean-radiant-temperature network method (Carroll 1980). This method is equivalent to putting all surfaces on a hypothetical sphere permitting each surface to have some view of every other surface. Compared with other contemporary computer programs, TARP is one of the few programs that handles the radiation exchange among interior surfaces and envelope surfaces. The heat-transfer coefficients at vertical interior surfaces, at horizontal interior surfaces with heat flow down, and at horizontal interior surfaces with heat flow up were taken as the constant values given in (ASHRAE, 1985).

The partition walls consisted of 2 x 4 in (50 x 100 mm) framing with 1/2 in (13 mm) gypsum board attached at opposite sides. The surface area of the partition walls was identical to the actual partition wall surface area of the Hastings' ranch house. Interior furnishings were modeled as a 2-in-thick (5 cm) slab of wood. The total weight of the interior furnishings was 7,000 lb (3,200 kg), and its specific heat was taken to be 0.29 Btu/lb•F (1,200 J/kg•K).

For the computer simulations, the thermostat was set at 68 F (20°C) for space heating and 76 F (24°C) for space cooling. Within the 8 F (4°C) range between the setpoints, space conditioning was not provided, and the test house was not ventilated. A constant internal load of 0.75 W/ft^2 of floor (8.1 W/m^2) was used to simulate heat release associated with occupancy.[1] The rate of air infiltration was taken to be constant at one volume change per hour.

RESULTS

Using climatic data from WYEC[2] computer tapes, annual space heating and cooling loads were predicted for the following cities: Madison, WI; Lake Charles, LA;

---

1 A special computer simulation with a diurnal occupancy profile having the same average value predicted very similar weekly space heating and cooling loads.

2 Weather Year for Energy Calculations (Crow 1981).

Washington, DC; Los Angeles, CA; and Charleston, SC. These cities were selected to represent the climates of the northern U.S., gulf coast, mid-atlantic, southern region of the west coast, and southeastern region of the United States, respectively.

Space Heating Load Correlations

Weekly average[1] space heating loads for the insulated house without interior surfaces (i.e., an empty building shell) located in Washington, DC are plotted as a function of average outdoor temperature in Figure 2A. Weekly averages were found to reduce scatter in the data due to variations in solar radiation and thermal mass effects. Note that when the outdoor temperature is below a break point of 47 F (8.3°C) and deviates from the balance point, the weekly heating loads follow a linear relationship. This break point was determined from a visual inspection of the plotted results. Here the term "balance point" denotes the outdoor temperature at which the heating load decreases to zero. When the average outdoor temperature is above this break point and near the balance point, the heating load departs from and lies above the linear relationship. In this nonlinear regime, the internal heat gains (i.e., solar and occupancy gains) cause the indoor temperature to rise above the thermostat setpoint temperature. As a result, the house is unable to utilize all of its internal heat gains, and its interior rejects thermal energy to the outdoor environment.

Interior surfaces (i.e., partition walls and furniture) were incorporated into the model of the building in two stages. First, surfaces without thermal storage capacity were added. Second, surfaces with thermal storage capacity were added.

The space heating load correlation for the case of interior surfaces without thermal storage is given in Figure 2B. The inclusion of interior surfaces without thermal storage increased the overall envelope heat-transfer coefficient by 3.0%. The overall envelope heat-transfer coefficient corresponds to the slope of the line. The inclusion of interior surfaces in the computer model for the house causes an interior envelope surface to view a higher radiant temperature (see Figure 3A), thereby increasing the rate of heat transfer at the surface.

The heating load correlation for the case of interior surfaces with thermal storage is given in Figure 2C. The addition of thermal storage to the interior surfaces produced a further increase of 1.9% in the overall envelope heat-transfer coefficient. This effect was believed to be due to the storage of solar energy in the interior surfaces, resulting in a further increase in the indoor radiant temperature. The thermal storage also caused the weekly heating loads near the balance point to more closely follow the linear relationship. The thermal storage considerably reduced overheating of the indoors during warm day periods. This increased the utilization of internal heat gains for space heating loads near the balance point. Under such a condition, the addition of more mass (i.e., wall mass) has been shown to have a small effect on annual space heating loads (Burch, Walton, Cavanaugh, and Licitra 1984).

Another interesting result is that the overall effect of including interior surfaces with thermal storage produced only a 0.5% increase in the annual heating load of the insulated residence located in Washington, DC. The overall effect

---

[1] It should be pointed out that the weekly averages are actually running averages over a 168-hour period (i.e., weekly averages with progressively shifted starting points).

is small because the individual effects on the overall envelope heat-transfer coefficient and the utilization of internal heat gains tend to offset each other. The impact of climate is considered later.

A similar set of results for the poorly insulated house is given in Figure 4. Here it is seen that the inclusion of interior surfaces increased the overall envelope heat-transfer coefficient by 12.6% compared to 4.9% for the insulated house. In the poorly insulated house, the inclusion of interior surfaces produces a larger change in the indoor radiant temperature (see Figure 3). Moreover, since the building envelope of the poorly insulated house contains smaller thermal resistance, changes in interior radiant temperature produce a larger effect on the overall envelope heat transfer.

In Figure 4, it is seen that the inclusion of interior surfaces in the modeling of the poorly insulated house did not have much effect on heating loads near the balance point.

Note that in Washington, DC the inclusion of interior surfaces with thermal storage produced a net increase in the annual space heating load of 0.5% in the insulated house and a net increase of 8.6% in the poorly insulated house. In the insulated house, the effect on the overall envelope heat-transfer coefficient and the effect on utilization of internal heat gains tend to offset each other. On the other hand, in the poorly insulated house, the effect on the overall envelope heat-transfer coefficient is the more dominant mechanism, resulting in a larger increase in the annual space heating load.

The exclusion of interior mass surfaces from computer predictions causes the benefits of envelope modifications for saving energy to be underestimated. This may be seen by considering the annual heating loads given in figures 2 and 4. Here it is seen that the evelope modifications resulted in a predicted savings of 3.01×10^7 Btu (3.18×10^{10} J) without interior surfaces and 3.49×10^7 Btu (3.68×10^{10} J) with interior surfaces, or a 14% difference.

An interesting adjunct to these results is that, when interior surfaces were included in the modeling of the house, most of the heating loads were well correlated by a linear relationship. Moreover, this linear relationship coincided closely with steady-state theory as shown in the next section.

Comparisons to Steady-State Theory

The space heating loads (Q_h) of a house with interior surfaces may be predicted using the relation:

$$Q_h = K \cdot (T_b - T_o) \tag{1}$$

Here T_o is the average outdoor temperature, and T_b is the balance-point temperature. The overall envelope heat-transfer coefficient (K) is given by:

$$K = \sum_{i=1}^{N} U_i \cdot A_i + \rho \cdot V \cdot I \cdot C_p \tag{2}$$

where $U_i \cdot A_i$ = thermal transmittance and surface area product for the i-th building component;

ρ = density of air;

V = volume of house;
I = rate of infiltration;
C_p = specific heat of air; and
N = total number of heat-transfer surfaces.

The balance-point temperature (T_b) is given by:

$$T_b = T_i - \frac{Q_i + Q_s - Q_e}{K} \tag{3}$$

Here T_i is the indoor temperature, Q_i and Q_s are the internal heat gains for occupany and solar, and Q_e is the earth heat loss that was treated as constant over the entire year.

Neglecting data near the balance point, the slope and T_b values derived from the heating load correlation were determined by regression analysis. The earth loss was determined to be 176 Btu/h (51.6 W) for the insulated house and 383 Btu/h (112 W) for the poorly insulated house. The solar gains (Q_s) for both houses were computed by the relation:

$$Q_s = \tau \cdot SC \sum_{i=1}^{4} A_i \cdot H_i \tag{4}$$

where A_i = surface area for windows for i-th orientation;
H_i = average incident solar radiation for i-th orientation;
τ = solar transmittance for DSA glass; and
SC = mean shading coefficient for window glazing.

The values for H_i were obtained from TARP. The mean shading coefficient was taken to be 0.81 for double-pane glazing and 0.92 for single-pane glazing. The solar transmittance for double-strength sheet (DSA) glass was taken to be 0.86. These values were evaluated at a 40° incident angle to represent mean daily performance.

The above steady-state model was used to predict the linear portion of the heating load correlations for both houses with interior surfaces. A comparison of the overall envelope heat-transfer coefficients and balance-point temperatures independently derived from the heating-load correlations and the steady-state theory are given in Table 4.

Since the overall envelope heat-transfer coefficients and balance-point temperatures derived independently from the heating load correlation and steady-state theory are in close agreement, it follows that the linear portion of the heating load correlations for both houses with interior surfaces is equivalent to steady-state theory.

Space Cooling Load Correlations

Space cooling load correlations for the insulated house located in Washington, DC are given in Figure 5A for the case without interior surfaces, in Figure 5B for the case of interior surfaces without thermal storage, and in Figure 5C for the case of interior surfaces with thermal storage. The inclusion of interior

surfaces produced a net increase in the effective overall envelope heat-transfer coefficient of 3.8% compared to 4.9% for the space heating load correlations. Here the term "effective overall envelope heat-transfer coefficient" denotes the rate of change of space cooling loads with outdoor temperature (i.e., the slope of a space cooling load correlation). Comparing Figures 5C and 5A, it is seen that the inclusion of interior surfaces only slightly affected space cooling loads near the balance point. An explanation is given below.

In the previous section dealing with space heating loads, the departure of weekly space heating loads from a linear relationship near the balance point was caused by the inability of the house to utilize all of its internal heat gains during warm day periods. In the case of the space cooling load correlations, the departure of weekly space cooling loads from a linear relationship near the balance point is believed to be due to the inability of the house to fully utilize all of the night cooling potential. For cooling days near the balance point, the outdoor temperature decreases well below the indoor setpoint temperature, and the house is naturally cooled at night by the outdoor environment. This causes the indoor temperature to decrease below the indoor setpoint temperature. The inclusion of interior surfaces produces only a small change in this temperature decline, thereby producing little effect on the space cooling loads.

From Figure 5C, it would appear that the linear portion of cooling load correlation departs from steady-state theory. That is, the slope of the correlation is 10.9% larger than the overall envelope heat-transfer coefficient given in Table 4. This peculiar behavior for the space cooling load correlation is not well understood, but it may be related to a variation in the utilization of the solar energy absorbed by the opaque surfaces of the building envelope with outdoor temperature.

A similar set of cooling load correlations for Washington, DC is given for the poorly insulated house in Figure 6. Here the inclusion of interior surfaces with thermal storage produced a net increase in the slope of the cooling load correlation of 12.7%, compared to 12.6% for the space heating load correlation.

A comparison of Figures 5C and 6C indicates that for the mild summer climate of Washington, DC the inclusion of insulation in the house had a small effect on the annual space cooling loads. It is seen that the annual cooling load for the poorly insulated house is only 5.2% above that for the insulated house. The effect is small because the insulation not only reduces the effective overall envelope heat-transfer coefficient but also decreased the balance-point temperature. A lower balance point caused more climatic periods to require space conditioning. These two effects tend to offset one another.

Impact of Climate

The effect of including interior surfaces in the computer model on annual space conditioning loads of the insulated house are summarized in Table 5 for the five climatic regions. The values represent the difference in space conditioning loads between the insulated house without interior surfaces and the identical house with interior surfaces.

The values may be understood by considering the distribution of average outdoor temperatures for the various climates. For instance, consider the space heating loads for the insulated house located in Madison, WI. Most of the heating days occur away from the balance point. In this situation, the effect of including interior mass surfaces on the overall envelope heat-transfer coefficient is approximately of equal magnitude to the effect on the utilization of internal

heat gains, and the two effects tend to offset each other. On the other hand, in a mild heating climate (such as the Gulf Coast, southeastern, or southern West Coast regions), most of the heating days are distributed near the balance point, where the increase in solar utilization is dominant. The net effect on the insulated house is a large percentage reduction in the prediction of the annual space heating load.

With regard to space cooling loads for the insulated house in hot climates, where the house operates predominantly away from the balance point, the effect on the effective overall envelope heat-transfer coefficient is the dominant mechanism, resulting in a net increase in prediction of the annual space cooling load. On the other hand, in mild climates, where the house operates predominantly near the balance point, space heating and cooling loads occur at different times of the day. In this situation, interior surfaces provide reductions in the prediction of both space heating and space cooling loads.

A similar set of results for the poorly insulated house is given in Table 6. Here the same considerations apply, except that interior surfaces produce a considerably larger increase in the overall envelope heat-transfer coefficient. This effect tends to dominate space conditioning loads, causing positive differences except in Los Angeles, CA where the house operated predominantly near the balance point.

These results indicate that the inclusion of interior surfaces in dynamic computer models has an important effect on the space conditioning loads of houses. The inclusion of interior surfaces produced differences ranging from 0.3% to 12%, except for the insulated house located in Los Angeles where it operated at the balance point.

Caviats and Cautions

The predicted effect of interior mass surfaces depends upon the way in which these surfaces are modeled in a computer program. It is the belief of the authors that the mean-radiant-temperature network model more closely approximates the thermal performance of the multi-room situation than other contemporary approximate models for interior mass surfaces. A strong need exists to investigate the relative accuracies of these different models.

SUMMARY AND CONCLUSIONS

In space heating applications, the inclusion of interior surfaces (i.e., partition walls and interior furnishings) in TARP Computer Program affected space conditioning loads in two ways: it increased the overall envelope heat-transfer coefficient in a linear regime away from the balance point and increased the utilization of internal heat gains in a nonlinear regime near the balance point. The effect on the overall envelope heat-transfer coefficient was observed to be considerably larger in the poorly insulated house. The effect on the overall envelope heat-transfer coefficient increased the annual heating load, while the effect on the utilization of internal heat gains decreased the annual heating load. The inclusion of interior surfaces in the modeling of the houses was observed to cause predicted space heating loads to approach steady-state theory.

In space cooling applications, the inclusion of interior surfaces increased the effective overall envelope heat-transfer coefficient in a linear regime away

from the balance point, but produced little change in space cooling loads in a nonlinear regime near the balance point. Thermal insulation in the building envelope was found to have a small effect in reducing annual space cooling loads. This was because the insulation produced a decrease in the balance-point temperature that tended to offset the increase in the effective overall envelope heat-transfer coefficient.

In computer predictions of annual space condition loads of the houses, including interior mass surfaces in the TARP Computer Program produced differences ranging from 0.3% to 12%, except for the insulated house located in Los Angeles where it operated at the balance point. The exclusion of interior mass surfaces from computer predictions cause the benefit of energy conserving modifications in houses to be underestimated.

REFERENCES

Anderson, B.; Bauman, F.; and Kammerud, R. 1980. Verification of BLAST by Comparison with Direct Gain Test Cell Measurments: Report No. LBL-10619. Lawrence Berkeley Laboratory, Nov.

Arumi-Noe, F. and Burch, D.M. 1984. "DEROB simulation of the NBS thermal mass test buildings." ASHRAE Transactions, 90, Pt. 2.

ASHRAE. 1985. ASHRAE Handbook--1985 Fundamentals. Atlanta: American Society of Heating, Refrigerating, and Air-Conditioning Engineers, Inc.

Burch, D.M.; Peavy, B.A.; and Powell, F.J. 1975. "Comparison between measured and computer-predicted hourly heating and cooling energy requirements for an instrumented wood frame townhouse subjected to laboratory tests." ASHRAE Transactions, 81, Pt. 2.

Burch, D.M.; Remmert, W.E.; Krintz, D.F.; and Barnes, C.S. 1982. "A field study of the effect of wall mass on the heating and cooling loads of residential buildings." Proceedings of the Building Thermal Mass Seminar. Oak Ridge National Laboratory, Conference 8206130, Oak Ridge, TN.

Burch, D.M.; Walton, G.N.; Cavanaugh, K.; and Licitra, B.A. 1984. "The effect of wall mass on annual heating and cooling loads of single family residences for five selected climates." Proceedings of the Symposium on Thermal Insulation Materials and Systems," Dallas, TX, Dec. 2-6.

Burch, D.M.; Krintz, D.F.; and Spain, R.S. 1984. "The effect of wall mass on winter heating loads and indoor comfort - an experimental study." ASHRAE Transactions, 90, Pt. 1.

Burch, D.M.; Davis, K.L.; Malcolm, S.A. 1984. "The effect of wall mass on the summer cooling of six test buildings." ASHRAE Transactions, 90, Pt. 2.

Burch, D.M.; Johns, W.L.; Jacobsen, T.; Walton, G.N.; and Reeve, C.P. 1984. "The effect of thermal mass on night temperature setback savings." ASHRAE Transactions, 90, Pt. 2.

Carroll, J.A. 1980. "An MRT method of computing radiant energy exchange in rooms." Proceedings of the 2nd Systems Simulation and Economics Analysis Conference, San Diego, CA.

Crow, L.W. 1981. "Development of hourly data for weather year for energy calculations (WYEC)." ASHRAE Journal, Vol. 23, No. 10, October.

Hastings, S.R. 1977. Three Proposed Typical House Designs for Energy Conservation Research: NBSIR-77-1309. National Bureau of Standards, Washington, D.C.

Judkoff, R.; Wortman, D.; and Burch, J. 1983. "Measured versus predicted performance of the SERI test house: a validation study." National Heat Transfer Conference, Seattle, WA, July.

Kusuda, T. 1976. NBSLD, the Computer Program for Heating and Cooling Loads of Buildings: Building Science Series 69. National Bureau of Standards, July.

Walton, G.W. 1980. Thermal Analysis Research Program-Reference Manual: NBSIR 88-2655. National Bureau of Standards, Washington, DC.

ACKNOWLEDGMENTS

This study was sponsored by the Department of Energy and the Electric Power Research Institute.

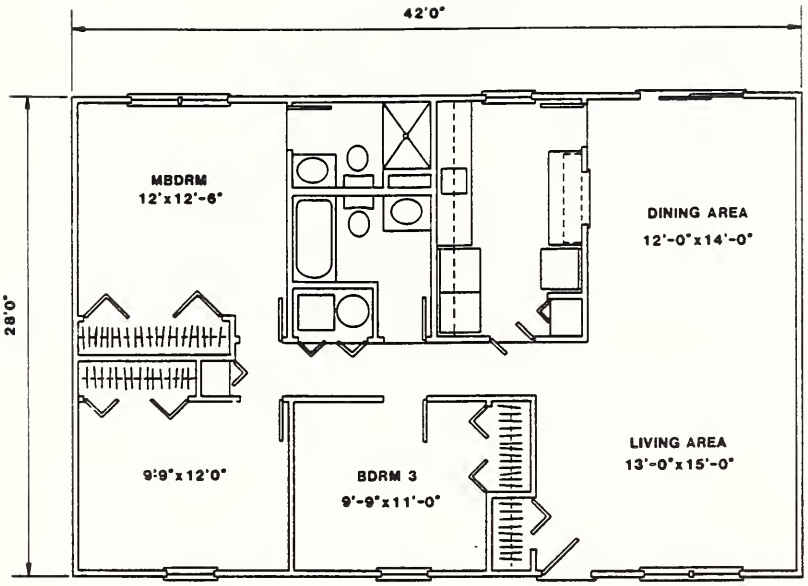

A. Floor plan

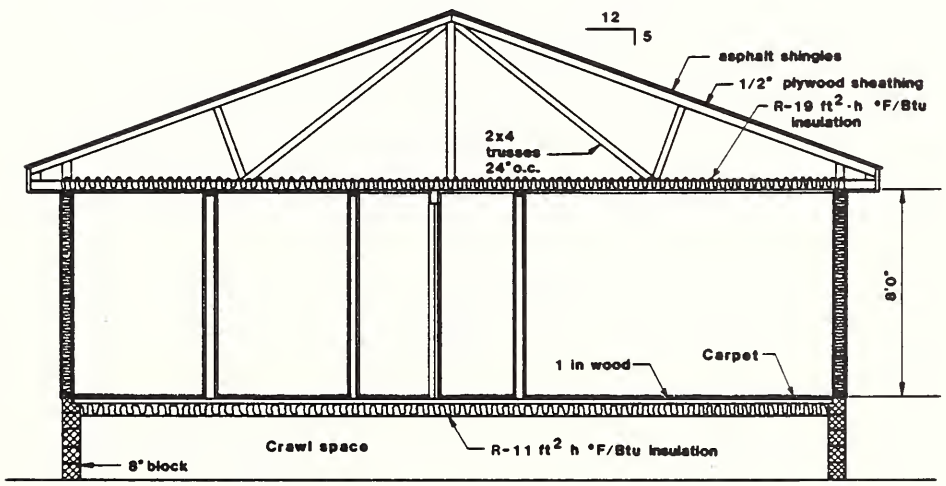

B. Elevation

Figure 1. Floor plan and elevation for the houses used in the analysis

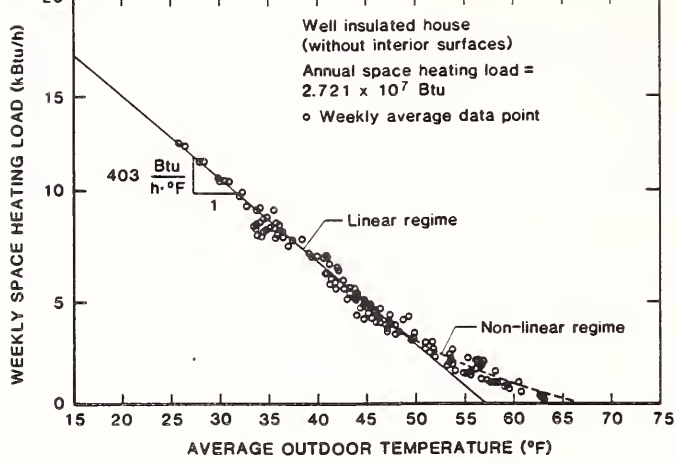

A. Without interior surfaces

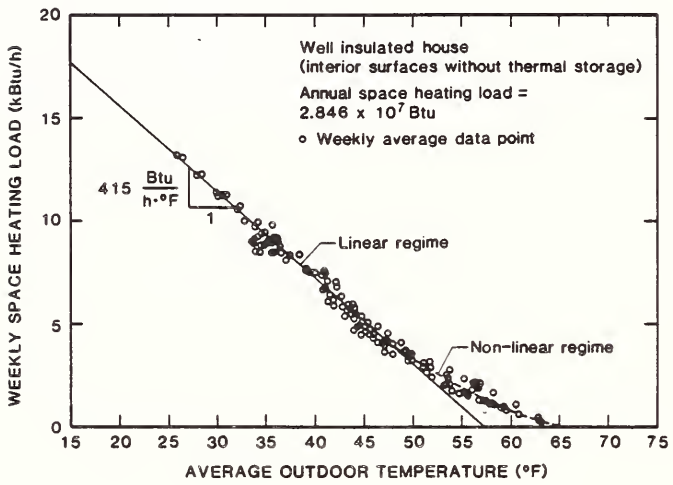

B. Interior surfaces without thermal storage

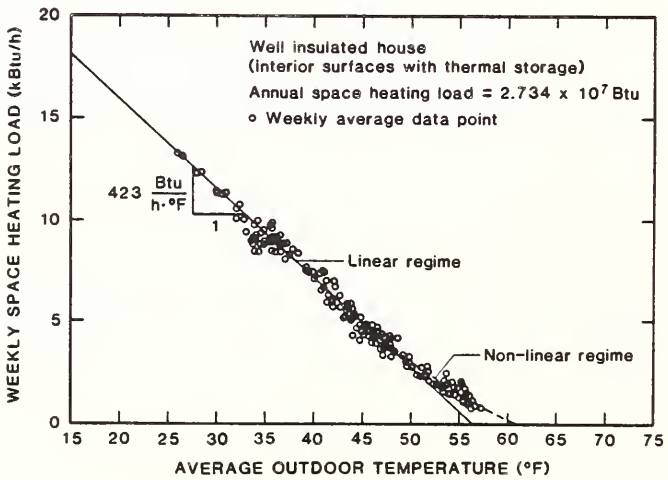

C. Interior surfaces with thermal storage

Figure 2. Heating load correlations for the insulated house located in Washington, DC

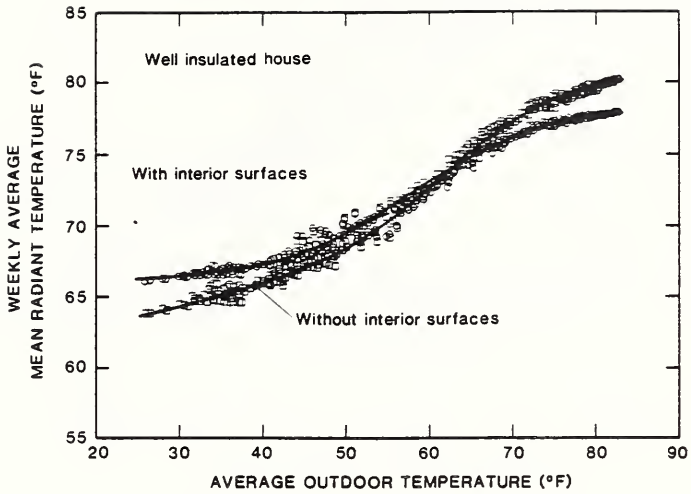

A. Insulated house

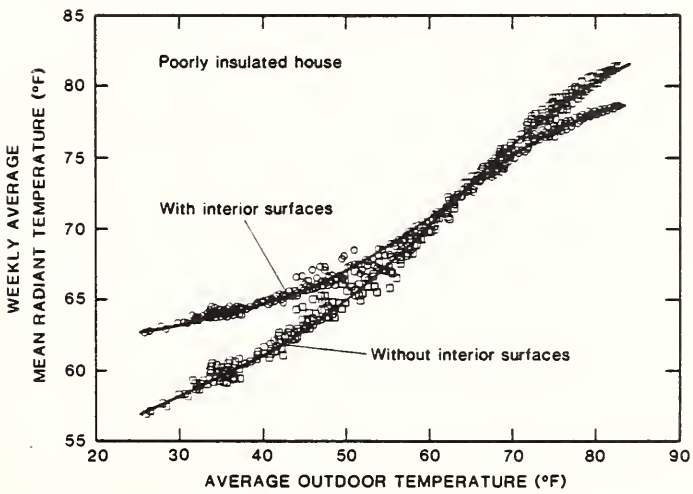

B. Poorly insulated house

Figure 3. Plot of the indoor mean-radiant temperature as a function of the average outdoor temperature

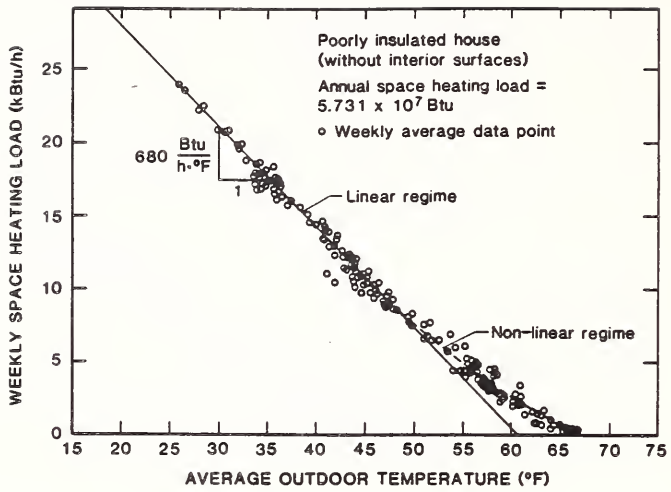

A. Without interior surfaces

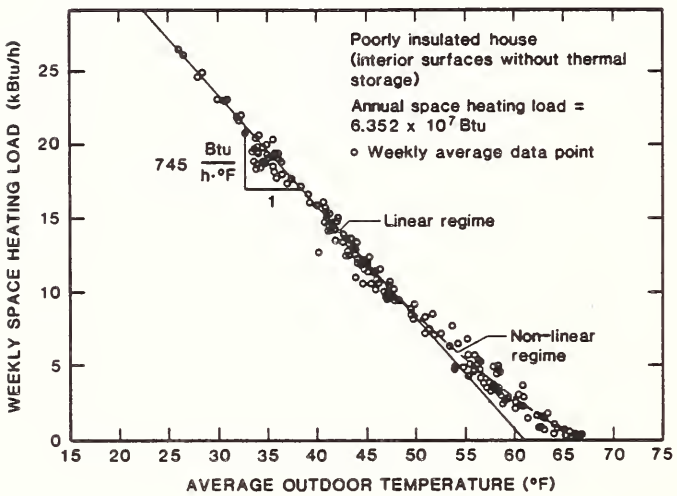

B. Interior surfaces without thermal storage

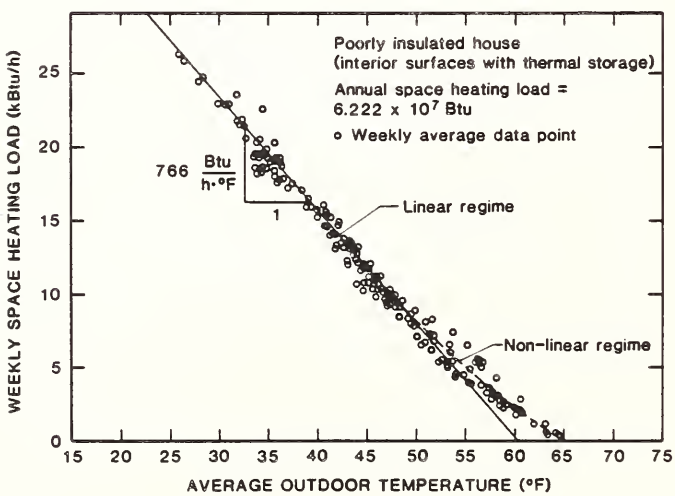

C. Interior surfaces with thermal storage

Figure 4. Heating load correlation for the poorly insulated house located in Washington, DC

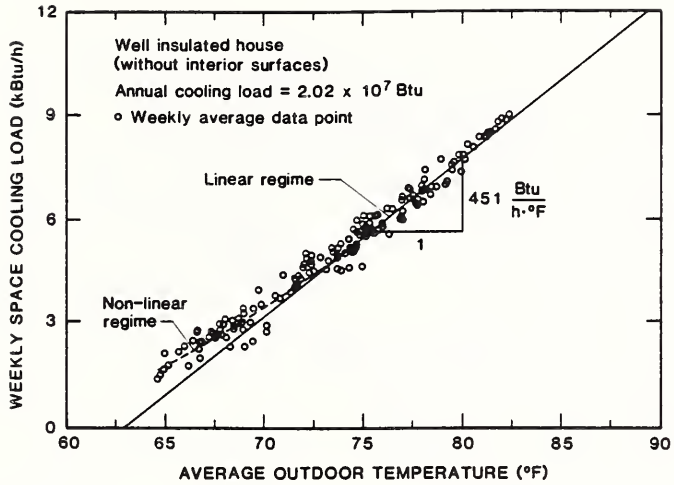

A. Without interior surfaces

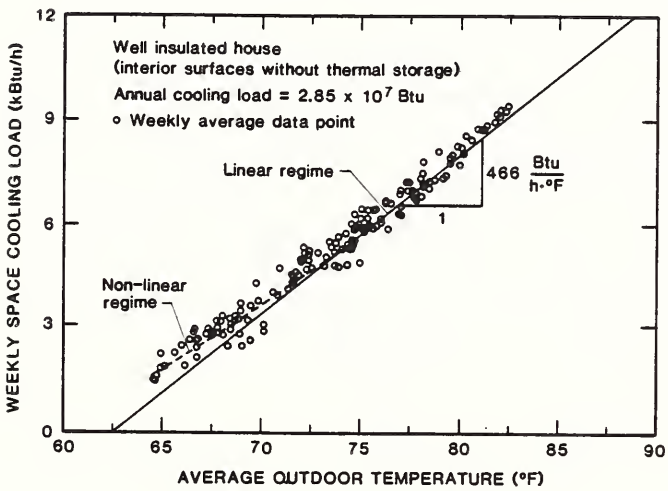

B. Interior surfaces without thermal storage

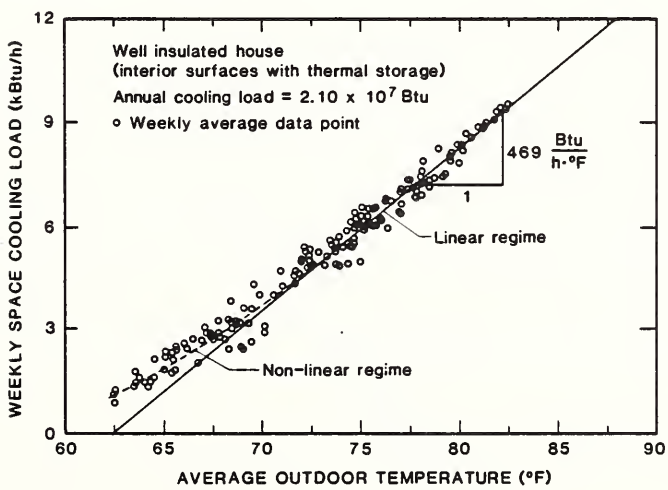

C. Interior surfaces with thermal storage

Figure 5. Cooling load correlations for the insulated house located in Washington, DC

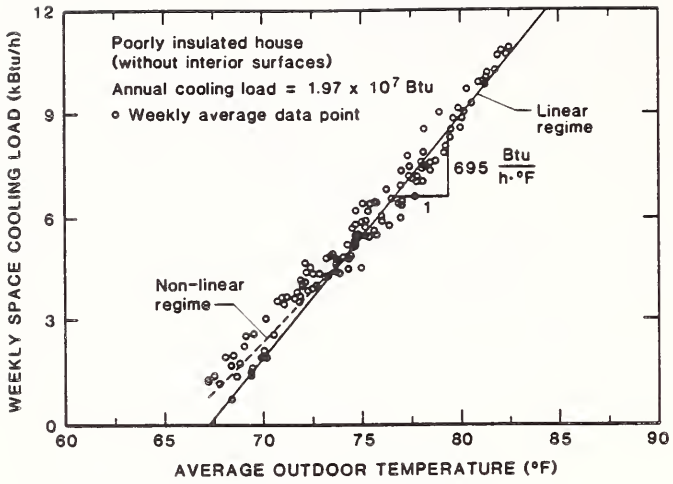

A. Without interior surfaces

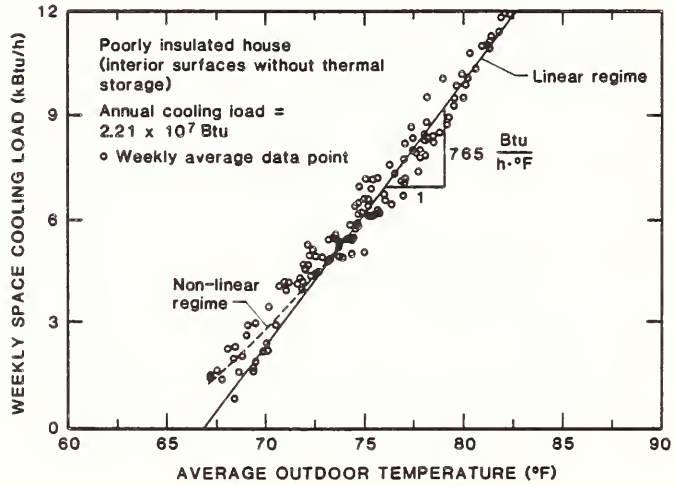

B. Interior surfaces without thermal storage

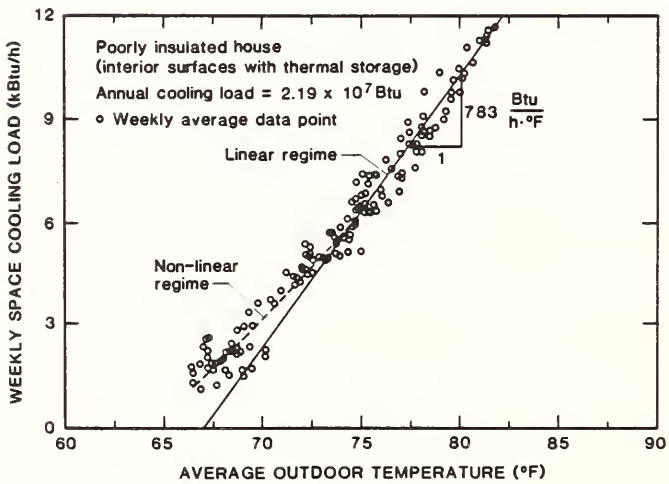

C. Interior surfaces with thermal storage

Figure 6. Cooling load correlations for the poorly insulated house located in Washington, DC

Table 1

Features of the Houses

Component	Insulated House	Poorly Insulated House
Glazing	Double Pane	Single Pane
Walls	R-11 Insulation	None
Ceiling	R-19 Insulation	R-11 Insulation
Floor	R-11 Insulation	None

Table 2

Heat-transfer Coefficients for the Insulated House

Component	Surface Area (A) ft^2	(m^2)	Thermal Transmittance (U) $Btu/h \cdot ft^2 \cdot F$	$(W/m^2 \cdot K)$	U·A Product $Btu/h \cdot F$	(W/K)
Glazing	141.	(13.1)	0.485	(2.75)	68.4	(36.0)
Walls	959.	(89.1)	0.083	(0.471)	79.6	(42.0)
Floor/Crawl space[1]					44.4	(23.4)
Ceiling/Attic					61.1	(32.2)
Door	20.1	(1.87)	0.285	(1.62)	5.7	(3.03)
Infiltration[2]					167.3	(88.2)
Overall Envelope Heat-Transfer Coefficient					426.5	(224.7)

[1] Calculated from 3-node model that included an air node, a bottom surface node, and top surface node. The bottom and top surfaces exchanged heat by radiation.

[2] Calculated from relation: $H_I = \rho \cdot V \cdot I \cdot C_p$, where ρ = density of air, V = volume, I = rate of infiltration, and C_p = specific heat of air.

Table 3

Heat-Transfer Coefficients for the Poorly Insulated House

Component	Surface Area (A) ft^2	(m^2)	Thermal Transmittance (U) Btu/h•ft^2•F	(W/m^2•K)	U•A Product Btu/h•F	(W/K)
Glazing	141.	(13.1)	0.961	(5.46)	135.5	(71.5)
Walls	959.	(89.1)	0.280	(1.59)	268.5	(141.0)
Floor/Crawl space[1]					96.6	(50.9)
Ceiling/Attic					76.4	(40.3)
Door	20.1	(1.87)	0.285	(1.62)	5.7	(3.01)
Infiltration[2]					167.3	(88.2)
Overall Envelope Heat-Transfer Coefficient					750.0	(395.)

[1] Calculated from 3-node model that included an air node, a bottom surface node, and top surface node. The bottom and top surfaces exchanged heat by radiation.

[2] Calculated from relation: $H_I = \rho \cdot V \cdot I \cdot C_p$, where ρ = density of air, V = volume, I = rate of infiltration, and C_p = specific heat of air.

Table 4

Comparison of TARP Predictions to Steady-State Theory

	Heating Load Correlation[1]				Steady-State Theory			
	K		T_b		K		T_b	
House	Btu/h•F	W/K	F	K	Btu/h•F	W/K	F	K
Insulated	423.	223.	58.1	14.5	427.	225.	57.3	14.1
Poorly Insulated	766.	404.	62.5	16.9	750.	396.	61.9	16.6

[1] predicted by TARP

Table 5

The Effect of Including Interior Mass Surfaces in Computer Model for the Insulated House

Climatic Region	City	Difference in Annual Space Conditioning Loads: Heating kWh	Heating %	Cooling kWh	Cooling %
Northern	Madison, WI	+46.9	+0.3	-99.6	-3.1
Mid Atlantic	Washington, DC	+38.1	+0.5	+234.	+4.0
Gulf Coast	Lake Charles, LA	-276.	-12.5	+357.	+3.6
Southeastern	Charleston, SC	-372.	-11.1	+173.	+2.1
Southern West Coast	Los Angeles, CA	-597.	-47.8	-431.	-10.2

Table 6

The Effect of Including Interior Mass Surfaces in Computer Model for Poorly Insulated House

Climatic Region	City	Difference in Annual Space Conditioning Loads: Heating kWh	Heating %	Cooling kWh	Cooling %
Northern	Madison, WI	2,549.	8.4	109.	4.3
Mid Atlantic	Washington, DC	1,439.	8.6	656.	11.4
Gulf Coast	Lake Charles, LA	202.	3.8	1,242.	11.7
Southeastern	Charleston, SC	314.	4.1	891	11.1
Southern West Coast	Los Angeles, CA	-366.	-8.5	-147.	-5.5

APPENDIX

EFFECT OF INTERIOR MASS SURFACES ON THE SPACE CONDITIONING LOADS OF TWO UNINSULATED TEST BUILDINGS

INTRODUCTION

Space heating and cooling load measurements for two uninsulated test buildings containing partition walls were conducted for winter, spring, and summer periods. One of the buildings had lightweight wood-frame wall construction, the other had heavyweight masonry wall construction. Some space cooling load measurements were conducted in the lightweight wood-frame building with additional interior mass in the form of office furniture. The weight of office furniture was selected to coincide with the weight of furniture per unit floor surface (i.e., 3.2 lb/ft^2 (16 kg/m^2)) typically found in residences. Office furniture was used instead of residential furniture because office furniture was available at no cost. The measured weekly space conditioning loads for these two buildings were plotted as a function of average outdoor temperature and compared to space conditioning load measurements without interior surfaces.

DESCRIPTION OF TEST BUILDINGS

Two 20 ft (6.1 m) by 20 ft (6.1 m) one-room test buildings with a 7-1/2 ft (2.3 m) high ceiling were constructed outdoors at the National Bureau of Standards location in Gaithersburg, MD.

These buildings had the same floor plan and orientation, and were identical except for the wall constructions which were as follows:

Building No. 2. Uninsulated lightweight wood frame; and
Building No. 4. Uninsulated masonry.

These buildings were used for the partition wall measurements described here, while the other buildings 1, 3, 5, and 6 were used for concurrent night temperature setback measurements (Burch, Johns, Walton, and Reeve 1984).

A detailed description of the exterior walls of buildings 2 and 4 is given in Table A-1.

The thermal resistances of the exterior walls of these buildings were designed to be equivalent but were actually somewhat different (see Table A-2). The exterior surfaces of buildings 2 and 4 were painted the same color paint so that they would have the same solar absorptance. An effort was made to make the construction of these two buildings representative of current practice in the United States.

Each building contained two double-hung windows on both the north and south walls. Each window contained an insulating glass window fitted with an exterior storm window. Each building had a 19.5 ft^2 (1.81 m^2) hollow metal door on the east wall filled with perlite insulation.

The edges of the concrete slab-on-grade floors were insulated with 1-in-thick (25 mm) polystyrene insulation at both the inner and outer surfaces of the footings. Two-inch-thick (50 mm) polystyrene insulation was placed over

Table A-1. Construction Details of Walls

Uninsulated Lightweight Wood Frame Building (No. 2)

0.5 in (13 mm) gypsum board
0.002 in (0.05 mm) polyethylene film
2 x 4 in (50 x 100 mm) studs placed 16 in (410 mm) o.c.
5/8 in (16 mm) exterior plywood

Uninsulated Masonry Building (No. 4)

0.5 in (13 mm) gypsum board
0.002 in (0.05 mm) polyethylene film
3/4 in (20 mm) air space created by 2 x 3/4 in (50 x 20 mm) furring strips placed 16 in (410 mm) o.c.
8 in (200 mm) 2-core hollow concrete block, 105 lb/ft^3 (1680 kg/m^3)

the top surfaces of the slab-on-grade floors in order to reduce the effect of seasonal variations in earth heat transfer.

Each building contained a pitched roof forming an attic space ventilated with soffit and gable vents. Eleven inches (280 mm) of glass-fiber blanket insulation (R-34 h·ft^2·F/Btu (R-6.0 m^2·K/W)) was installed over the ceiling.

Each building contained a centrally located 4.1 kW electric forced-air heating plant equipped with a 13,000 Btu/h (3,800 W) split, vapor-compression, residential air-conditioning system.

A description of the instrumentation and measuring technique is given in references (Burch, Krintz, and Spain 1984 and Burch, Davis, and Malcolm 1984).

DESCRIPTION OF INTERIOR MASS SURFACES

An east/west interior partition wall containing a standard-size door opening was installed in buildings 2 and 4 (see Figure A-1). The partition wall divided the interior of each building into north and south rooms having approximately equal floor area. The partition walls consisted of 2 x 4 in (5 x 10 cm) studs with 1/2 in (1.3 cm) gypsum board installed at opposite sides. The total wall cross-section framed was 27 ft^2 (2.5 m^2) out of a total partition wall cross-section of 145 ft^2 (13.5 m^2), giving a framing fraction of 19%. Each of the rooms was served by separate supply and return ducts that provided approximately equal volumes of conditioned air to each space. The thermostat for controlling the heating/cooling plant was located 5 ft above the floor at the north side of the partition (see Figure A-1). The interior surfaces of the building including the partition walls were painted with an off-white latex paint.

For some of the summer tests, 1,280 pounds (581 kg) of office furniture was installed in the lightweight wood-frame building (No. 2).

HEAT-TRANSFER PROPERTIES

The walls of the test buildings had a surface area of 523 ft^2 (48.6 m^2). The thermal resistances and thermal masses of the exterior walls of buildings

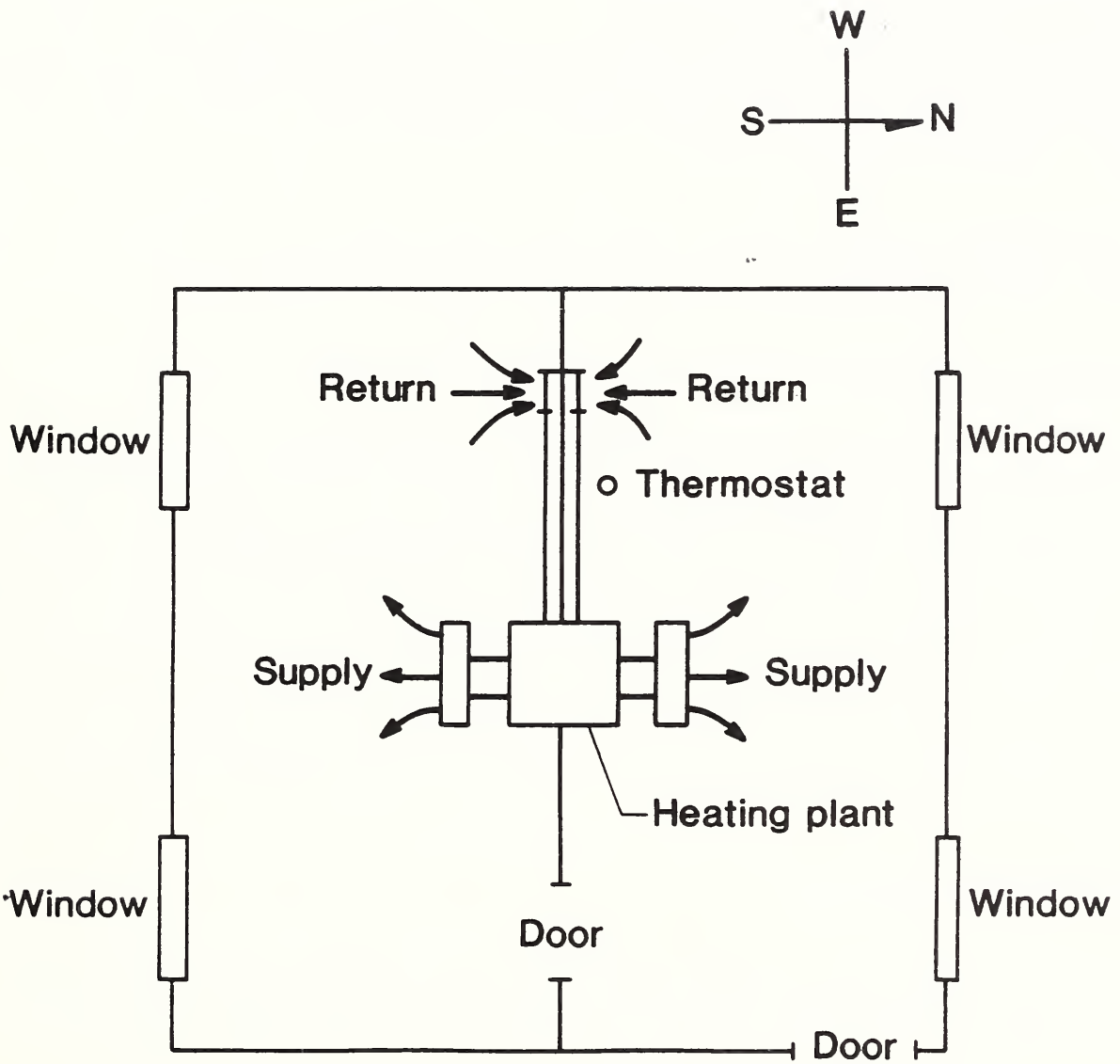

Figure A-1. Schematic drawing showing location of the partition wall

Table A-2. Heat-Transfer Properties for the Test Buildings

Building No.	Walls			Envelope Heat-Transfer Coefficient (K)	
	Thermal Resistance[1] (R) $h \cdot ft^2 \cdot F/Btu$	$m^2 \cdot K/W$	Mass lb/ft^2	Btu/h·F	W/K
2	3.6	0.63	4.2	184.	97.0
4	4.6	0.81	42.	151.	79.6

[1] Air-to-air thermal resistance.

2 and 4 are summarized in Table A-2. The thermal resistances were determined by guarded-hot-box measurements decribed in (Burch et al. 1982). The heat transfer properties for other parts of the building are given in (Burch et al. 1982).

The thermal capacitance $(\rho \cdot V \cdot C_p)$[2] was determined to be 248 Btu/F (4.71×10^5 J/K) for the partition walls in each building and about 270 Btu/F (5.13×10^5 J/K) for the office furniture.

EXPERIMENTAL PROCEDURE

Space heating and cooling load measurements of the two test buildings without interior mass surfaces were conducted during 1982. For these measurements, the windows were maintained in a closed position, and a constant internal load of 290 W was maintained within each building. Fixed thermostat settings of 68 $\pm$ 0.5 F (20 $\pm$ 0.3°C) for space heating and 76 $\pm$ 0.5 F (24 $\pm$ 0.3°C) for space cooling were used during the tests. The test buildings were not opened, except when technicians entered each day to collect data and check internal loads. A similar series of measurements was conducted with partition walls installed in the two buildings during 1983. During a portion of the summer of 1983, office furniture was installed in the lightweight insulated wood-frame building (No 2). The space heating and space cooling tests are summarized in Table A-3.

METHOD OF NORMALIZING DATA

In order to provide a meaningful correlation between measured heating loads and outdoor temperature, it was necessary to account for the effect of solar loading, indoor temperature, and earth temperature variations. The normalization procedure is described below.

The daily electric load (Q_e) expressed in Btu/h (W) supplied to each building during periods requiring space heating was fitted to an equation of the form:

---

[2] Here $(\rho \cdot V \cdot C_p)$ is product of density, volume, and specific heat.

Table A-3. Summary of Space Heating and Cooling Tests

Test Description	Test Period	Number of Weeks
Tests without partition walls		
• Winter	Jan. 4 - April 11, 1982	14.0
• Spring	April 12 - May 2, 1982	3.0
• Summer	July 26 - Aug. 17, 1982	3.0
Tests with partition walls		
• Winter	Feb. 3 - April 1, 1983	8.1
• Spring	April 11 - May 3, 1983	3.1
• Summer	July 18 - Aug. 26, 1983	5.6
• Summer (with office furniture)	Aug. 31 - Sept. 6, 1983	3.9

$$Q_e = K \cdot (T_i - T_o) - \beta \cdot H + D \qquad \text{(A-1)}$$

where

K = envelope heat-transfer coefficient, Btu/h·F (W/K);

$T_i - T_o$ = daily average inside-to-outside temperature difference, F (K);

H = daily average solar radiation incident on a south facing vertical surface, Btu/h·ft^2 (W/m^2); and

K, β, and D = regression coefficients.

After the winter heating season measurements were completed, normalized heating loads (Q_h') were determined from the relation:

$$Q_h' = Q_e - Q_i + \beta \cdot (H - H') - K \cdot (T_i - T_i') + U_f \cdot A_f \cdot (T_g - T_g') \qquad \text{(A-2)}$$

where

Q_i = constant internal load for the building, Btu/h (W);

T_i = intended indoor temperature, F (K);

T_g' = average ground temperature during test period, F (K);

U_f = thermal transmittance of floor slab, Btu/h·ft^2·F, (W/m^2·K);

A_f = surface area of floor slab, ft^2 (m^2); and

H' = mean daily-average solar vertical radiation, Btu/h·ft^2 (W/m^2).

The normalized heating load (Q_h') is the heating load that would have occurred if the indoor temperature (T_i) were maintained at T_i' = 68 F (20°C), the daily average solar radiation (H) were maintained at H' =35.3 Btu/h·ft^2 (111 W/m^2), and the earth temperature (T_g) beneath the floor slabs were maintained at

$T_g' = 56.1$ F (13.4°C).

A similar procedure was used to obtain meaningful correlations between space cooling loads and outdoor temperature.

RESULTS

Winter Season

Normalized weekly space heating loads measured during the winter heating season are plotted as a function of average outdoor temperature in Figure A-2(A) for the uninsulated wood-frame building and in Figure A-2(B) for the uninsulated masonry building. In each figure, the open circles depict points without a partition wall, while the solid circles depict points with a partition wall. The solid line is a linear regression of the data without a partition wall. The slope of the straight line is the envelope heat-transfer coefficient (K), and its horizontal-axis intercept is the balance-point temperature (T_b). Note that in both buildings little difference exists between the measured loads with and without a partition wall.

Spring Season

Daily space heating loads measured during the spring heating season are compared to steady-state theory in Figure A-3(A) for the uninsulated wood-frame building (No. 2) and in Figure A-3(B) for the uninsulated masonry building (No. 4). In each figure, the quantity (Q_h/K) is plotted as a function of the temperature difference (T_b-T_o). Here measured values for the envelope heat-transfer coefficient (K) and balance-point temperature (T_b) determined from a regression analysis of measured heating loads for the winter heating season (see Figure A-2(A) and (B)) were used in the analysis. Data without a partition wall are depicted with open circles, and data with a partition wall are depicted with solid circles. As in the case of winter results, very little difference exists between data with and data without a partition wall.

Summer Season

A similar set of results was prepared for the summer cooling test (see Figure A-4). Data for the uninsulated masonry building (No. 4) with both partition walls and office furniture are depicted with a symbol "Δ". As in the case of the previous results, no consistent difference can be attributed to the presence of partition walls and office furniture.

COMPUTER ANALYSIS

The Computer Program TARP, described in the main body, was used to predict space heating and space cooling loads for the uninsulated wood-frame and uninsulated masonry test buildings. For this analysis, an operation schedule coinciding to the manner in which the buildings were operated was specified as input to TARP.

Space Heating Loads

Computer-predicted space heating loads are plotted as a function of outdoor temperature for the uninsulated wood-frame building (No. 2) in Figure A-5. The

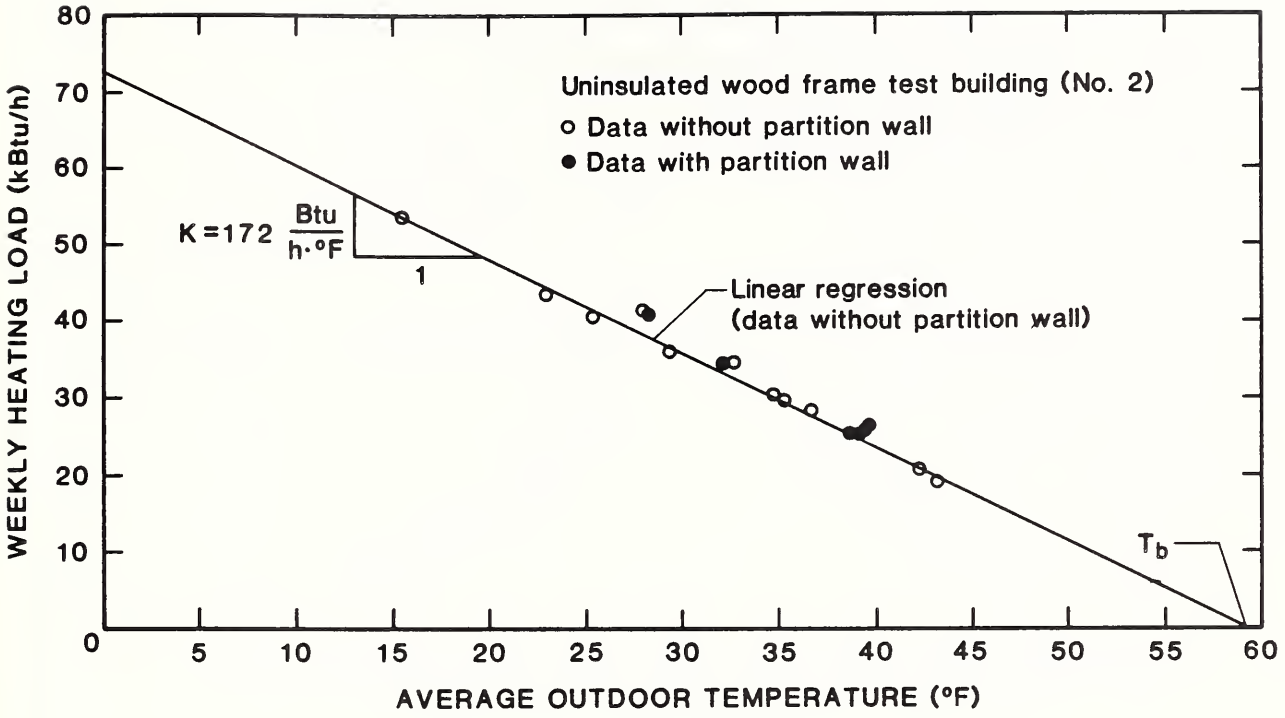

A. Uninsulated wood-frame test building (No. 2)

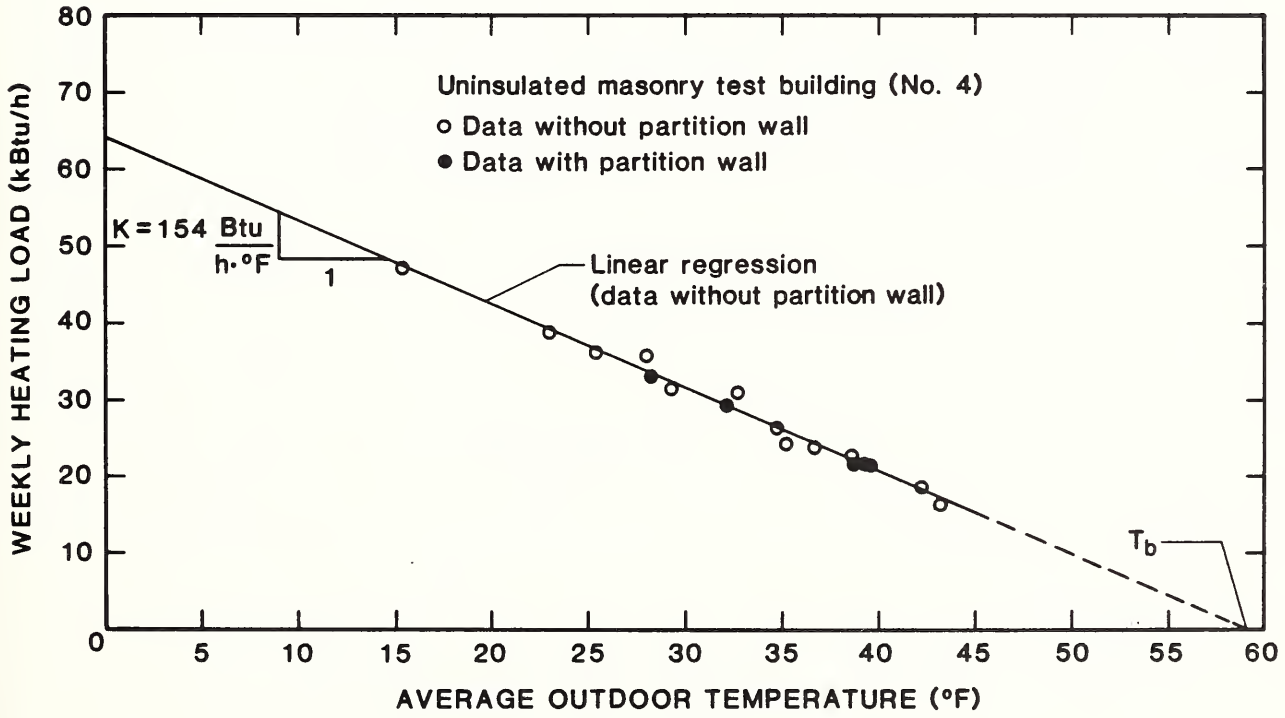

B. Uninsulated masonry test building (No. 4)

Figure A-2. Average weekly space heating loads measured during the winter season

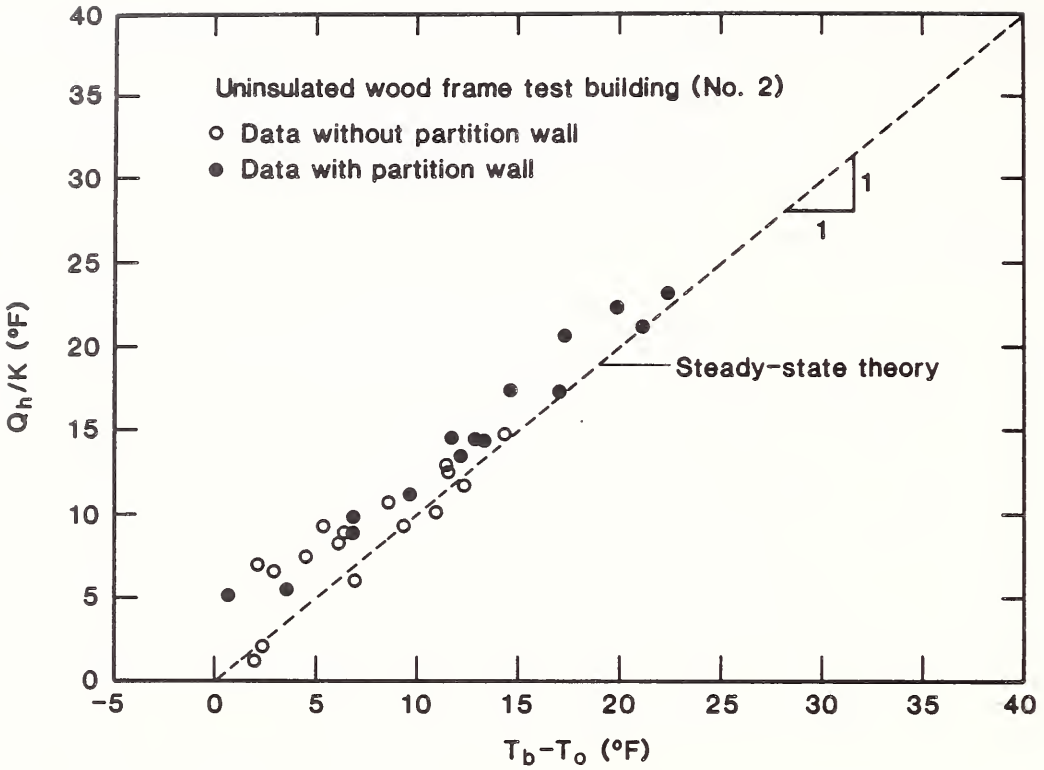

A. Uninsulated wood-frame test building (No. 2)

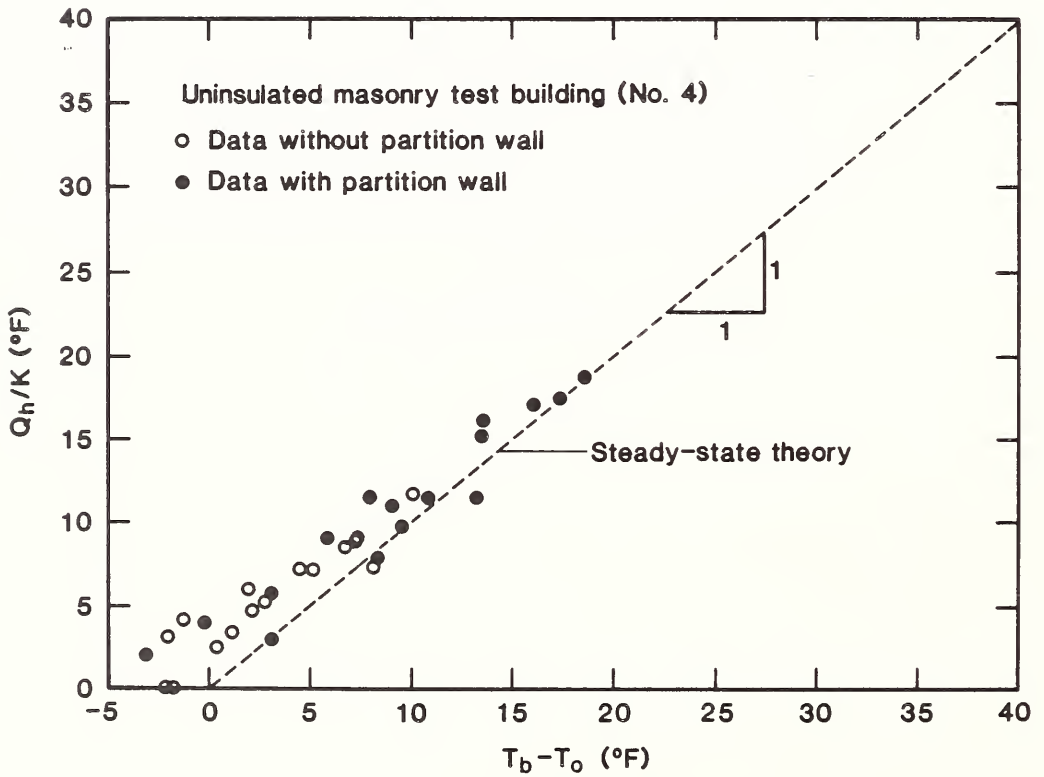

B. Uninsulated masonry test building (No. 4)

Figure A-3. Daily space heating loads measured during the spring season

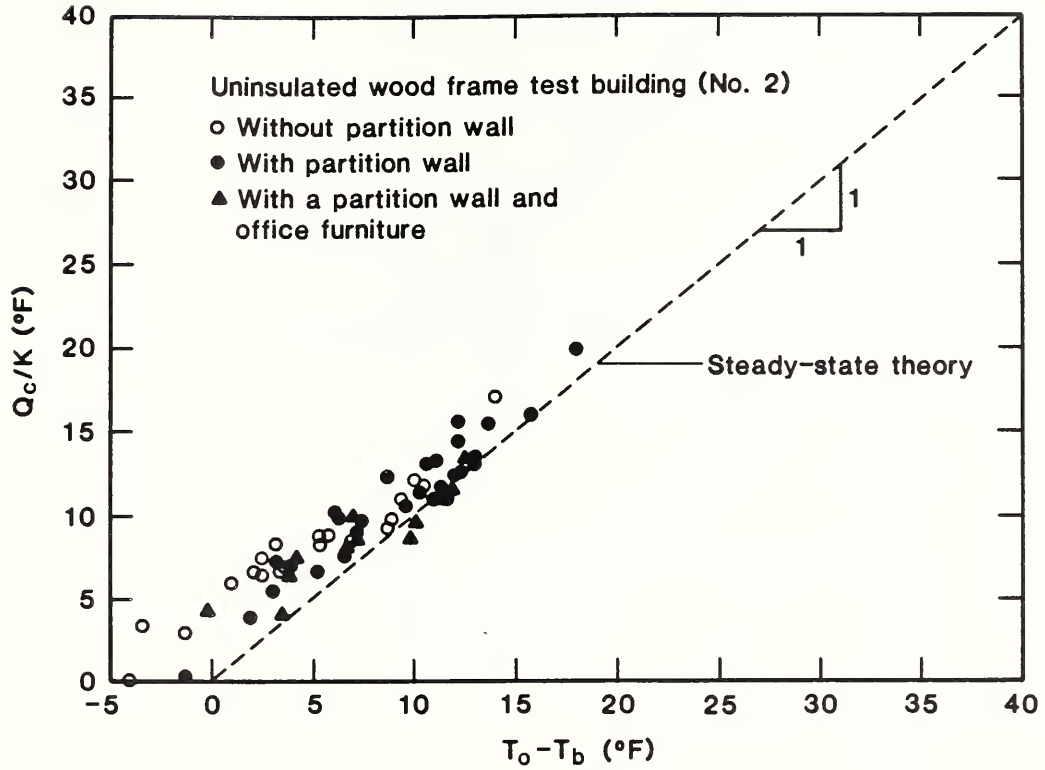

A. Uninsulated wood-frame test building (No. 2)

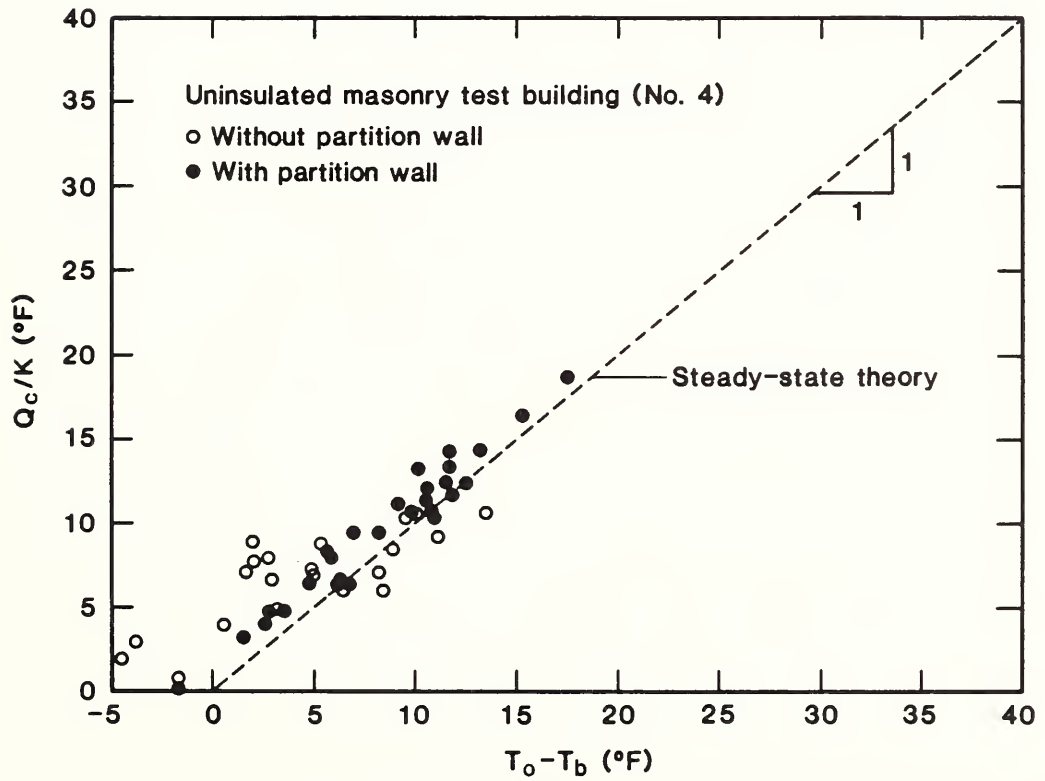

B. Uninsulated masonry test building (No. 4)

Figure A-4. Daily space cooling loads measured during the summer season

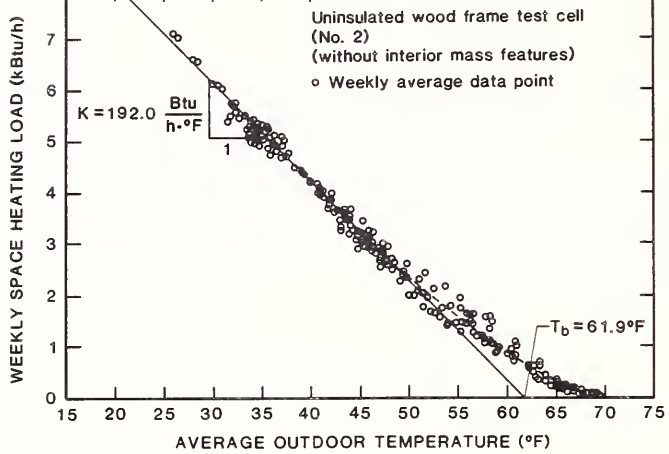

A. Without interior surfaces

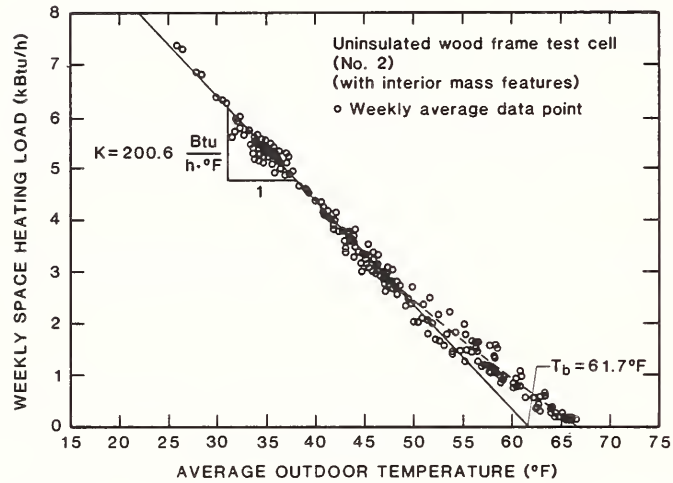

B. With interior surfaces

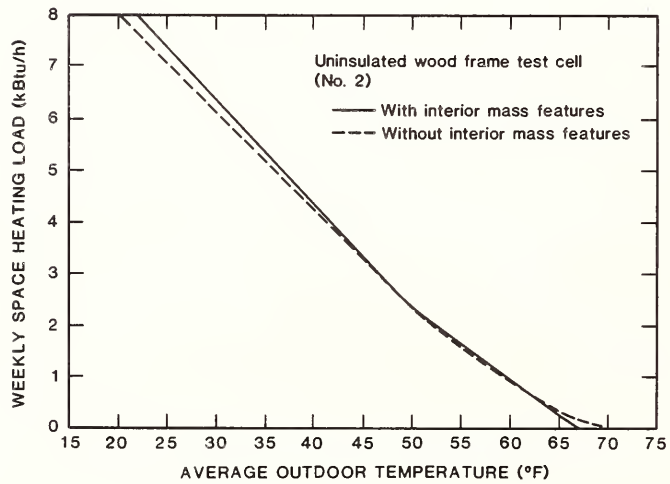

C. Comparison of curves

Figure A-5. Predicted space heating load plotted as a function of outdoor temperature for the insulated wood-frame test building (No. 2)

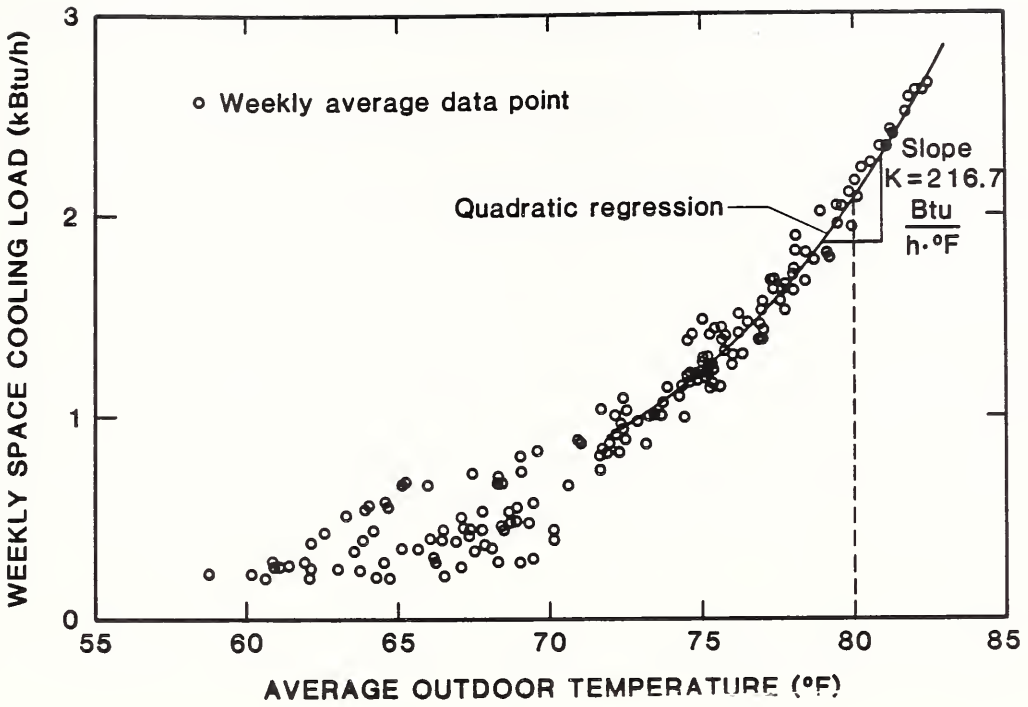

A. Without interior surfaces

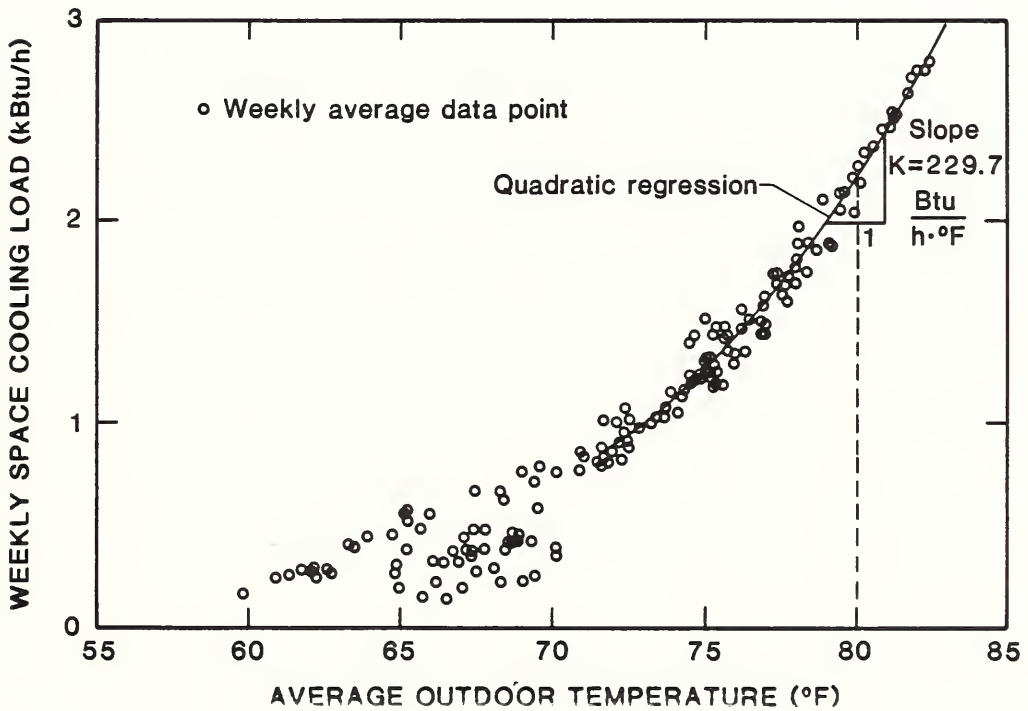

B. With interior surfaces

Figure A-6. Predicted space cooling load plotted as a function of the average outdoor temperature for the uninsulated wood-frame test building (No. 2)

results without the interior mass surfaces are given in Figure A-5(A). A similar set of results with interior surfaces including both partition wall and the office furniture is given in Figure A-5(B). The heating load correlations with and without interior mass features are compared in Figure A-5(C).

The results indicate that the presence of interior surfaces has a very small effect on space heating loads for these test buildings. Based on these results, it is not surprising that the field measurements did not detect significant differences attributable to the interior surfaces.

Space Cooling Loads

Computer-predicted space cooling load correlations for the uninsulated wood-frame test building (No 2) are given in Figure A-6. These results indicate that the presence of interior surfaces has a very small effect on space cooling loads. It would have been extremely difficult to measure such small differences. Note that the weekly average space cooling loads are fitted with good agreement to a quadratic equation. These results indicate that the space cooling loads depart from the linear steady-state theory.

A similar analysis for the uninsulated masonry test building (No. 4) was carried out. The results were very similar to those for the uninsulated wood-frame test building (No. 2).

Explanation for Small Effect

Interior surfaces in the uninsulated test buildings had a smaller effect on space conditioning loads compared to the poorly insulated house described in the main body of the paper. This was because the solar gains were comparatively small and the envelope thermal resistance was comparatively large in the uninsulated test buildings. Small solar gains caused the presence of interior surfaces to exert little differences on the utilization of these solar gains. The interior surfaces of the walls viewed a radiant temperature not much different than the indoor air temperature due to the large thermal resistance in other parts of the building envelope. Therefore, the presence of interior surfaces produces only a very small increase in the envelope heat transfer coefficient.

SUMMARY AND CONCLUSIONS

A comprehensive series of field measurements were conducted to investigate the effect of interior mass surfaces (i.e., a partition wall and furnishings) on the space conditioning loads of a lightweight wood-frame and a heavyweight masonry uninsulated test buildings. The presence of these interior surfaces produced no consistent differences in space heating and cooling loads. Computer-predictions of the performance of these test buildings corroborated the field measurements. The effect of interior surfaces in the uninsulated test buildings was small chiefly because other parts of the building envelopes, except for the walls, had relatively large thermal resistance, and the solar gains were small.

NBS-114A (REV. 2-8C)

U.S. DEPT. OF COMM. BIBLIOGRAPHIC DATA SHEET (See instructions)	1. PUBLICATION OR REPORT NO. NBSIR 86-3377	2. Performing Organ. Report No.	3. Publication Date MAY 1986

4. TITLE AND SUBTITLE

THE EFFECT OF INTERIOR MASS SURFACES ON THE SPACE HEATING AND COOLING LOADS OF A SINGLE-FAMILY RESIDENCE

5. AUTHOR(S)

D. M. Burch, G. N. Walton, K. Cavanaugh and B. A. Licitra

6. PERFORMING ORGANIZATION (If joint or other than NBS, see instructions)

NATIONAL BUREAU OF STANDARDS
DEPARTMENT OF COMMERCE
WASHINGTON, D.C. 20234

7. Contract/Grant No.

8. Type of Report & Period Covered

9. SPONSORING ORGANIZATION NAME AND COMPLETE ADDRESS (Street, City, State, ZIP)

Department of Energy
Electric Power Research Institute

10. SUPPLEMENTARY NOTES

☐ Document describes a computer program; SF-185, FIPS Software Summary, is attached.

11. ABSTRACT (A 200-word or less factual summary of most significant information. If document includes a significant bibliography or literature survey, mention it here)

A computer program called TARP is used to analyze the effect of interior mass surfaces (i.e., partition walls and interior furnishings) on the weekly space heating and cooling loads of a well insulated and a poorly insulated residence.

When the outdoor temperature deviated from the balance point, the inclusion of interior mass surfaces in the modeling of the houses increased the interior radiant temperature. This, in turn, increased the envelope heat-transfer coefficient for the houses. This effect was found to be more significant in the poorly insulated house compared to the well insulated house. When the outdoor temperature was near the balance point, the thermal storage provided by interior surfaces caused the internal heat gains to be more effectively utilized, and weekly space heating loads tended to approach a "high mass limit" that coincided with steady-state theory. Under this condition, additional mass has only a small effect on space heating loads. The results of this study indicated that significant errors can occur when interior mass surfaces are excluded from dynamic computer simulations of residences.

12. KEY WORDS (Six to twelve entries; alphabetical order; capitalize only proper names; and separate key words by semicolons)

whole building performance; interior mass surfaces; thermal mass; computer-predicted building performance; and steady-state theory.

13. AVAILABILITY

☒ Unlimited

☐ For Official Distribution. Do Not Release to NTIS

☐ Order From Superintendent of Documents, U.S. Government Printing Office, Washington, D.C. 20402.

☒ Order From National Technical Information Service (NTIS), Springfield, VA. 22161

14. NO. OF PRINTED PAGES

35

15. Price

$9.95